

## IRRADIATION SPECTRUM AND IONIZATION-INDUCED DIFFUSION EFFECTS IN CERAMICS — S. J. Zinkle (Oak Ridge National Laboratory)

### SUMMARY

There are two main components to the irradiation spectrum which need to be considered in radiation effects studies on nonmetals, namely the primary knock-on atom energy spectrum and ionizing radiation. The published low-temperature studies on  $\text{Al}_2\text{O}_3$  and  $\text{MgO}$  suggest that the defect production is nearly independent of the average primary knock-on atom energy, in sharp contrast to the situation for metals. On the other hand, ionizing radiation has been shown to exert a pronounced influence on the microstructural evolution of both semiconductors and insulators under certain conditions. Recent work on the microstructure of ion-irradiated ceramics is summarized, which provides evidence for significant ionization-induced diffusion. Polycrystalline samples of  $\text{MgO}$ ,  $\text{Al}_2\text{O}_3$ , and  $\text{MgAl}_2\text{O}_4$  were irradiated with various ions ranging from 1 MeV  $\text{H}^+$  to 4 MeV  $\text{Zr}^+$  ions at temperatures between 25 and 650°C. Cross-section transmission electron microscopy was used to investigate the depth-dependent microstructure of the irradiated specimens. Dislocation loop nucleation was effectively suppressed in specimens irradiated with light ions, whereas the growth rate of dislocation loops was enhanced. The sensitivity to irradiation spectrum is attributed to ionization-induced diffusion. The interstitial migration energies in  $\text{MgAl}_2\text{O}_4$  and  $\text{Al}_2\text{O}_3$  are estimated to be  $\leq 0.4$  eV and  $\leq 0.8$  eV, respectively for irradiation conditions where ionization-induced diffusion effects are expected to be negligible.

### RESULTS AND DISCUSSION

Numerous microstructural studies of radiation effects in ceramics have been performed over the past 35 years, utilizing a variety of irradiation sources including electrons, ions and neutrons [1-3]. In order to make quantitative comparisons between data obtained with different irradiation sources, the effects of irradiation spectrum (along with other important experimental variables such as temperature and dose rate) need to be considered. Two main components of the irradiation spectrum must be considered for nonmetals. First, the energy spectrum of primary knock-on atoms (PKAs) produced by elastic collisions can affect the efficiency of point defect production, in a manner analogous to that commonly observed in metals. Second, inelastic collisions (electronic ionization and subthreshold atomic collisions) may affect point defect recombination and diffusion. As noted later in this paper, ionization effects often appear to be more important than PKA spectrum effects in irradiated ceramics.

Figure 1 compares measurements of the surviving defect fraction (displacement damage efficiency) in  $\text{Al}_2\text{O}_3$  and Al as a function of the average PKA energy [4-9]. The data have been normalized to the calculated displacements per atom (dpa) according to the Norgett-Robinson-Torrens (NRT) modified Kinchin-Pease formula. Most of the data on  $\text{Al}_2\text{O}_3$  were obtained from optical absorption measurements of oxygen monovacancy (F center) concentrations, and therefore are a lower limit to the total surviving defect fraction. Further details are discussed elsewhere [10]. The data for Al show a monotonic decrease in surviving defect fraction with increasing PKA energy, which is similar to the behavior observed in numerous other metals. Considerable scatter exists in the corresponding  $\text{Al}_2\text{O}_3$  data, but the measurements do not exhibit any apparent dependence on PKA energy. As reviewed elsewhere, the surviving defect fraction data for  $\text{MgO}$  also appear to be insensitive to PKA energy, with an average value of ~30% [10]. There are several possible explanations for the weak dependence of the surviving defect fraction of PKA energy in  $\text{MgO}$  and  $\text{Al}_2\text{O}_3$ . Some studies suggest that the spontaneous recombination volume for close Frenkel pairs in these materials may be much larger than typical values in metals [11,12]. This would produce efficient recombination of point defects produced by low

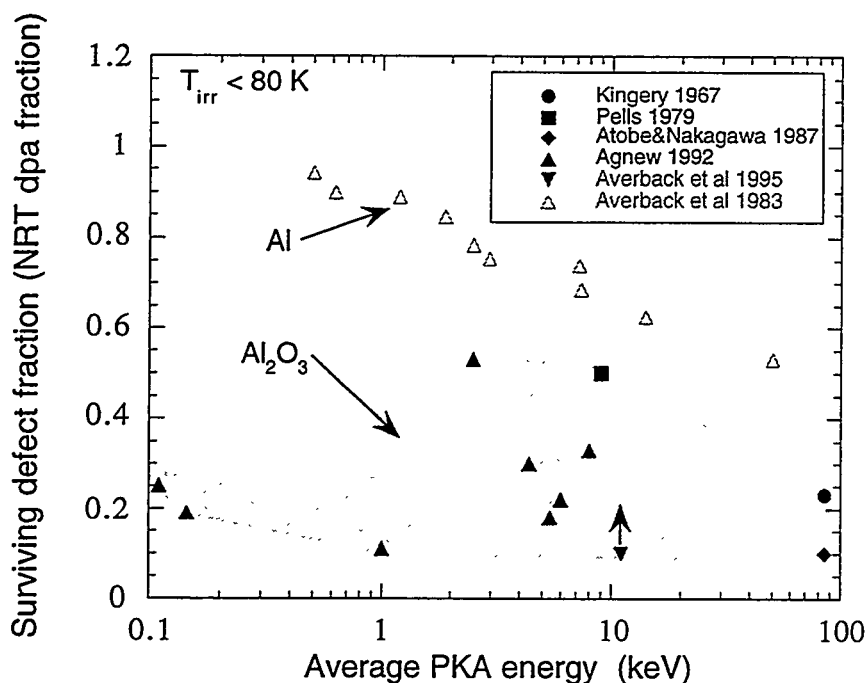


Fig. 1. Comparison of the defect production efficiency in  $\text{Al}_2\text{O}_3$  [4-7] and Al [9].

energy PKAs, since their average separation distance could be comparable to the spontaneous recombination distance. However, molecular dynamics calculations on MgO indicate that the spontaneous recombination volume is only slightly larger than typical values for metals [13]. It has also been noted that the low atomic mass and high melting point of  $\text{Al}_2\text{O}_3$  would inhibit the formation of the dense displacement cascades which are responsible for the decrease in displacement damage efficiency in metals at high PKA energies [7]. Rigorous analysis of the experimental data base is hampered by a lack of information on interstitial migration energies in MgO and  $\text{Al}_2\text{O}_3$  [10]. Several studies suggest that interstitials in  $\text{Al}_2\text{O}_3$  may be mobile at temperatures below 80 K (corresponding to migration energies of 0.2 to 0.8 eV) [4,14], whereas other authors have concluded that interstitial migration only occurs at temperatures above 300 K with migration energies as high as 1.8 eV [7,15]. All of the  $\text{Al}_2\text{O}_3$  data in Fig. 1 at PKA energies <10 keV are from Agnew [7], who performed irradiations at ~80 K. If interstitials in  $\text{Al}_2\text{O}_3$  are mobile at 80 K, point defect recombination could explain the low measured values of the surviving defect fraction in  $\text{Al}_2\text{O}_3$  compared to the Al data. The Al data were obtained at temperatures <10 K, where interstitials are immobile.

Another possible explanation for the low measured surviving defect fractions in MgO and  $\text{Al}_2\text{O}_3$  at low PKA energies is associated with ionization-induced migration and recombination of point defects [16-18]. It is worth noting that typical low-PKA energy irradiation sources such as electrons and light ions produce high amounts of ionization per dpa. Therefore, if ionization-induced diffusion processes are operating, the relative importance of ionization-induced point defect recombination would be highest for the irradiation sources which were used to generate the low-PKA energy data.

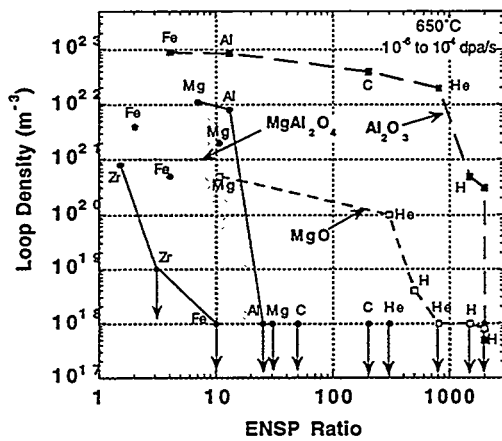


Fig. 3. Effect of ENSP ratio on the loop density in ion-irradiated ceramics.

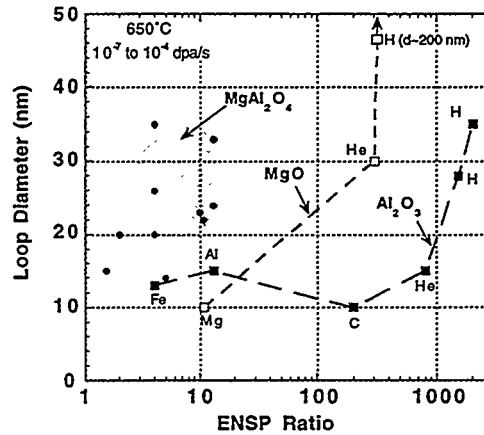


Fig. 4. Effect of ENSP ratio on the loop size in ion-irradiated ceramics.

Measurements of the dislocation loop size and density were performed on cross-section TEM specimens of  $\text{MgAl}_2\text{O}_4$ ,  $\text{Al}_2\text{O}_3$  and  $\text{MgO}$  following ion irradiation at  $650^\circ\text{C}$ . Quantitative measurements were typically obtained at one or two depths in regions that were at least  $0.3\ \mu\text{m}$  from the irradiated surface and implanted ion region. Both  $\text{MgO}$  and  $\text{Al}_2\text{O}_3$  were found to be relatively insensitive to variations in the ion mass for ions heavier than He. However, dramatic decreases in the midrange dislocation loop density occurred in  $\text{MgO}$  and  $\text{Al}_2\text{O}_3$  for helium ion and proton irradiations, respectively. Figures 3 and 4 summarize the loop density and size measurements as a function of the ENSP ratio for the 3 ceramics irradiated with different MeV ions at  $650^\circ\text{C}$  at damage rates between  $10^{-6}$  and  $10^{-3}$  dpa/s. Measurements were typically obtained at several depths (with corresponding different ENSP ratios) for each type of ion, as labeled in Figs. 3 and 4. A sharp decrease in the loop density occurred in  $\text{MgAl}_2\text{O}_4$  for ENSP ratios greater than  $\sim 10$ . The corresponding critical ENSP ratios for  $\text{MgO}$  and  $\text{Al}_2\text{O}_3$  were  $\sim 500$  and  $\sim 1500$ , respectively. Further work is needed to establish the effect of temperature and dose rate on these critical ENSP values. The loop density and size were only weakly dependent on the ENSP ratio below the critical value. It is noteworthy that the loop size increases significantly in the same position where the loop density sharply decreases. The decrease in loop density and concomitant increase in loop size (coarsening) above a critical ENSP ratio is indicative of enhanced point defect diffusion, according to standard chemical rate theory. The increase in loop size associated with the decrease in loop density indicates that ionization-induced diffusion is the principle mechanism responsible for the irradiation spectrum effect. However, it is also possible that ionization-enhanced point defect recombination may be contributing to the observed sensitivity to irradiation spectrum.

The dislocation loop data for spinel exhibits a transition from a high density of small loops to a low density of large loops for ENSP ratios of  $\sim 2$  to  $\sim 20$  for different ions, suggesting that there may be an underlying PKA spectrum effect. However, most of the scatter in the spinel data disappears if the loop parameters are plotted vs. the ratio of the total ionization per unit damage energy (TI-DE). An analysis of the data plotted in Figs. 3 and 4 indicates that the critical TI-DE ratio for spinel is  $\sim 15$ , corresponding to  $\sim 60$  electron-hole pairs per dpa. The corresponding critical TI-DE ratios for  $\text{MgO}$  and  $\text{Al}_2\text{O}_3$  are  $\sim 1000$  and  $2000$ , respectively ( $\sim 4000$  and  $\sim 10^4$  electron-hole pairs per dpa).

In summary, it appears that the observed irradiation spectrum effect on the microstructure of ion irradiated oxide insulators is primarily associated with ionization-induced diffusion processes. Both vacancy and interstitial diffusion appear to be promoted by ionizing radiation. However, the possibility that PKA energy spectrum and ionization-enhanced point defect recombination processes may be exerting some influence on the microstructural evolution cannot be discounted. A brief overview of ionization-induced point defect diffusion processes is given in the following section.

As discussed elsewhere, very little is known about the interstitial migration energies in  $\text{Al}_2\text{O}_3$  and  $\text{MgAl}_2\text{O}_4$  [10]. Several radiation effects studies on  $\text{Al}_2\text{O}_3$  have suggested that interstitial migration does not occur until temperatures of ~300 and 700 K for the oxygen and aluminum sublattices, respectively [7,19], which corresponds to an activation energy of ~1.6 eV for the slower defect (Al in this case). Conversely, Kingery [4] concluded that interstitial migration occurred in  $\text{Al}_2\text{O}_3$  with a range of activation energies between 0.2 and 0.8 eV. A rough estimate of the migration energy of the rate-determining (slower) interstitial for the cation and anion sublattices can be determined from measurements of the width of the denuded zone adjacent to internal sinks such as grain boundaries in irradiated materials. As shown elsewhere [20], the width of the loop denuded zone (L) adjacent to a point defect sink can be derived from simple chemical rate theory equations in the limiting case of high sink densities ( $C_s > 10^{14}/\text{m}^2$ ) to be

$$L = \frac{D_i C_i^{\text{crit}} \sqrt{C_s}}{P} \quad (2)$$

where P is the displacement damage rate,  $D_i$  is the interstitial diffusivity, and  $C_i^{\text{crit}}$  is the threshold matrix interstitial concentration to produce observable dislocation loop nucleation. Chemical rate theory models for metals have found that  $C_i^{\text{crit}} \sim 10^{-14}/\text{atom}$  [21]. In this simple analysis, it is assumed that the presence of a denuded zone is indicative of an insufficient interstitial concentration on both the anion and cation sublattices (i.e., it is assumed that the increased sink strength associated with cluster nucleation by the slower-moving interstitial species would lead to capture of the faster-moving interstitial species and subsequent stoichiometric interstitial loop formation). Using this assumption, the interstitial diffusivity in Eq. 2 is associated with the slower-moving interstitial species. Based on microstructural measurements [20,22] of the midrange loop sink strength and the grain boundary denuded zone width of 15 nm for  $\text{Al}_2\text{O}_3$  irradiated with 2-MeV  $\text{Al}^+$  ions at 650°C, the estimated interstitial diffusivity is  $\sim 10^{-10} \text{ m}^2/\text{s}$ . This corresponds to a migration energy of ~0.8 eV, assuming typical values for the pre-exponential factor (Eq. 1). It should be noted that impurity trapping effects may have reduced the effective interstitial mobility in the denuded zone width measurements. Therefore, the migration energy of ~0.8 eV is likely an upper limit to the intrinsic (impurity-free) value in  $\text{Al}_2\text{O}_3$ . This estimate of the interstitial migration energy is subject to considerable uncertainty, particularly since the value of  $C_i^{\text{crit}}$  is not reliably known. However, the migration energy of  $\leq 0.8$  eV for the slower-moving interstitial species appears to be in reasonable agreement with the measurement by Kingery [4]. Further support that the migration energy for the slower-moving anion or cation interstitial is ~0.5-1 eV in  $\text{Al}_2\text{O}_3$  comes from TEM observations that faulted interstitial dislocation loops were readily formed during 4 MeV  $\text{Ar}^+$  ion irradiation at 300 K, whereas resolvable loops were not detected in specimens irradiated at 200 K to the same dose of 10 dpa [23,24].

The migration energy for the slowest interstitial species in  $\text{MgAl}_2\text{O}_4$  can be estimated using the same technique. For example, using the measured loop sink strength and the grain boundary denuded zone width of 250 nm [20] for spinel irradiated with 2-MeV  $\text{Al}^+$  ions under identical conditions to that used for the alumina specimen, the estimated diffusivity is

$\sim 10^{-8}$  m<sup>2</sup>/s. This corresponds to a migration energy of  $\sim 0.4$  eV. Once again, this is likely an upper limit to the intrinsic migration energy of the slowest interstitial species, since impurity trapping effects may have reduced the effective interstitial mobility in the experimental measurements. There are no known measurements of interstitial migration energies in spinel with which this estimate can be compared.

### Summary of Ionization-Induced Diffusion Processes

The pronounced coarsening in the dislocation loop microstructure above a critical value of the ENSP ratio, along with the absence of dislocation loops in ionization-rich irradiation environments, suggest that the observed irradiation spectrum dependence in the three oxide ceramics (Figs. 3,4) may be primarily associated with ionization-induced diffusion effects. According to simple chemical rate theory, the steady state concentration of point defects ( $C_{i,v}$ ) is proportional to  $P/(D_v C_s)$  and  $P/(D_i C_s)$  for vacancies and interstitials, respectively for sink-dominant conditions, where  $C_s$  is the sink strength and  $P$  is the displacement damage rate [25,26]. The corresponding steady state concentrations for point defect recombination-dominant conditions are proportional to  $(P/D_v)^{1/2}$  and  $(PD_i/D_i^2)^{1/2}$  for vacancies and interstitials, respectively. Therefore, for both sink- and recombination-dominant conditions, the matrix point defect concentrations are reduced for high diffusivities. If the point defect concentration falls below the critical level needed to produce significant loop nucleation ( $\sim 10^{-14}$ /atom for interstitials), then dislocation loops would not be observed in the irradiated region.

Several different mechanisms for enhanced point defect diffusion associated with ionizing radiation have been proposed for nonmetals [16,17,27,28]. The "electrostriction" mechanism is based on the possibility that a high concentration of electron-hole pairs in the conduction band may alter the bond lengths (local lattice parameter) and consequently the point defect migration energy. The "energy release" mechanism assumes that electron-hole pair recombination (or energy released by de-excitation of an excited state) may provide sufficient thermal energy to induce point defect migration. These two diffusion mechanisms are discussed in detail elsewhere [16,17,27,28] and will not be considered further. The "normal ionization-enhanced diffusion" mechanism (more appropriately called "normal IID") is based on the concept that a point defect in an ionized charge state may have a significantly lower migration energy compared to a non-ionized defect. A final intriguing diffusion mechanism is the "Bourgoin-Corbett" (bistable defect) mechanism. In this mechanism, athermal point defect migration is possible if the stable site for the ionized charge state corresponds to the migration saddle point for the non-ionized defect charge state, and vice versa.

The bistable defect configuration has been reported for Si and Ge interstitials [17]. Recent calculations for oxygen interstitial migration in MgO indicate that the ground state lattice position is (111) dumbbell and the O<sup>2-</sup> lattice position is the cube centered site, with the lowest energy saddle point for the O<sup>2-</sup> interstitial being the (111) dumbbell [29]. Therefore, ionization-induced athermal migration via the Bourgoin-Corbett mechanism appears to be possible for the MgO oxygen interstitial. Corresponding calculations for the Mg sublattice in MgO or for the point defects in Al<sub>2</sub>O<sub>3</sub> or MgAl<sub>2</sub>O<sub>4</sub> are not available. Oxygen vacancy migration in MgO or Al<sub>2</sub>O<sub>3</sub> via the Bourgoin-Corbett mechanism does not appear to be possible, since quantum chemical calculations indicate that non-ionized and ionized vacancies occupy the same lattice site in these materials [30,31]. A simple estimate of the magnitude of point defect diffusion possible via the Bourgoin-Corbett mechanism can be obtained by assuming that the rate-limiting step is ionization of the point defect (i.e., by assuming that the time for the ionized defect to reacquire a free electron and return to the ground state is negligible) and by assuming that point defect ionization by capture of migrating holes is negligible. Assuming random-walk diffusion in a simple cubic lattice, the

diffusion coefficient can be written as  $D \sim 1/6 a^2 \Gamma$ , where  $\Gamma$  is the jump frequency (point defect ionization frequency) and  $a$  is the jump distance associated with the two hops by the ionized and ground state defect (roughly equal to the lattice parameter). The atomic ionization frequency in MgO for a typical medium-mass ion beam current of  $\sim 1 \mu\text{A}/\text{cm}^2$  ( $\sim 1 \text{ MGy/s}$  ionizing dose rate) is  $\Gamma \sim 0.01$  ionizations/atom-s, assuming a bandgap energy of 10 eV. The resultant diffusion coefficient for this ionizing dose rate is  $D \sim 2 \times 10^{-22} \text{ m}^2/\text{s}$ , which would produce a minuscule random-walk diffusion distance of  $\sim 1 \text{ nm}$  in 1 hour.

From this simple calculation, it appears that the Bourgoin-Corbett bistable defect mechanism would generally produce negligible amounts of long-range interstitial migration in MgO for most experimental irradiation conditions. On the other hand, this athermal defect migration mechanism would be an efficient method for correlated "close-pair" point defect recombination. This IID mechanism also offers a possible explanation for the observed amorphization resistance of irradiated MgO at low temperatures, since it is unlikely that the critical levels of atomic disordering (chemical mixing) necessary to induce amorphization could be achieved if close-pair point defect recombination occurred readily. This mechanism may also be responsible for the observed sublinear accumulation rate of oxygen vacancies (F centers) in MgO irradiated at 4 K with 2.2 MeV electrons [12]. Since the maximum irradiation dose of  $< 0.001 \text{ dpa}$  was too low for saturation of the defect density to occur, the sublinear accumulation rate suggests that athermal impurity or oxygen interstitial migration (with resultant uncorrelated point defect recombination) may have occurred.

Several studies have obtained evidence that ionized point defects in semiconductors [16,17] and insulators [29] may have a lower migration energy than non-ionized defects, as proposed by the "normal IID" mechanism. The calculations for MgO indicate that the migration energies for ionized oxygen interstitials and vacancies may be 40 to 80% of the ground state migration energies [29,30]. A key uncertainty for quantification of the amount of diffusion possible via this mechanism is the lifetime of the ionized point defect. If the point defect rapidly reacquires an electron during migration through the lattice then, by analogy with the preceding Bourgoin-Corbett mechanism calculation, the "normal IID" mechanism would not produce a significant contribution to long-range diffusion. Ionized point defect lifetimes of  $> 1 \mu\text{s}$  would generally be necessary to produce significant long-range diffusion for typical ion irradiation conditions in ceramic insulators.

## CONCLUSIONS

Published surviving defect fraction (production efficiency) measurements for MgO and  $\text{Al}_2\text{O}_3$  show a surprisingly weak dependence on PKA energy, with a typical value of  $\sim 30\%$  of the modified Kinchin-Pease displacements for PKA energies between  $\sim 0.1$  and 100 keV. It is possible that ionization-induced diffusion processes associated with the ionization-rich low PKA energy irradiations (electrons, light ions) may have caused correlated (and uncorrelated) point defect recombination and thereby produced an underestimate of the "intrinsic" stable defect production rate at low PKA energies.

Significant irradiation spectrum effects have been observed in dislocation loop microstructures of ion-irradiated MgO,  $\text{Al}_2\text{O}_3$  and  $\text{MgAl}_2\text{O}_4$ . Loop formation is inhibited for irradiation with light ions. The sensitivity to irradiation spectrum appears to be primarily associated with ionization-induced diffusion effects, although PKA spectrum and ionization-enhanced point defect recombination effects may also be playing a role. Additional data obtained at different temperatures and dose rates, along with rate theory modeling, are needed in order to better understand the physical processes responsible for the observed dependence of the microstructure on irradiation spectrum.

The rate-limiting interstitial migration energies for  $\text{Al}_2\text{O}_3$  and  $\text{MgAl}_2\text{O}_4$  are estimated to be  $\sim 0.8$  eV and  $\sim 0.4$  eV, respectively for irradiation conditions where ionization-induced diffusion should not have a strong influence. Ionization-induced diffusion is expected to reduce these migration energies, but calculated values for the migration energies of ionized point defects are not available for either of these two materials.

## REFERENCES

- [1] L.W. Hobbs, *J. Amer. Ceram. Soc.* 62 (1979) 267.
- [2] F.W. Clinard, Jr. and L.W. Hobbs, in *Physics of Radiation Effects in Crystals*, eds. R.A. Johnson and A.N. Orlov (Elsevier Science Publishers, Amsterdam, 1986) p. 387.
- [3] L.W. Hobbs, F.W. Clinard, Jr., S.J. Zinkle and R.C. Ewing, *J. Nucl. Mater.* 216 (1994) 291.
- [4] W.D. Kingery, *J. Nucl. Mater.* 24 (1967) 21.
- [5] G.P. Pells, A.E.R.E. Harwell Report AERE-R9359 (1979).
- [6] K. Atobe and M. Nakagawa, *Cryst. Latt. Def. Amorph. Mater.* 17 (1987) 229.
- [7] P. Agnew, *Nucl. Instr. Meth. B* 65 (1992) 305.
- [8] R.S. Averback, P. Ehrhart, A.I. Popov and A.v. Sambreek, *Rad. Effects Def. Solids* 136 (1995) 169.
- [9] R.S. Averback et al., *J. Nucl. Mater.* 113 (1983) 211.
- [10] S.J. Zinkle and C. Kinoshita, *J. Nucl. Mater.* (1997) in press.
- [11] A.E. Hughes, *J. Physique* 34, Colloque C9 (1973) 515.
- [12] C. Scholz and P. Ehrhart, in *Beam Solid Interactions: Fundamentals and Applications*, MRS Symposium Proceedings vol. 279, eds. M. Nastasi et al. (Materials Research Society, Pittsburgh, 1993) p. 427.
- [13] T. Sonoda, C. Kinoshita and Y. Isobe, *Annales de Physique* 20, Colloque C3 (1995) 33.
- [14] R.T. Cox, *Phys. Lett.* 21 (1966) 503.
- [15] T.D. Gulden, *Philos. Mag.* 15 (1967) 453.
- [16] J.C. Bourgoin and J.W. Corbett, *Rad. Effects* 36 (1978) 157.
- [17] J.C. Bourgoin, *Rad. Effects Def. Solids* 111&112 (1989) 29.
- [18] L.C. Kimerling, *Solid-State Electronics* 21 (1978) 1391.
- [19] G.P. Pells, *Rad. Phys. Chemistry* 22 (1983) 1053.
- [20] S.J. Zinkle, in *15th Int. Symp. on Effects of Radiation on Materials*, ASTM STP 1125, eds. R.E. Stoller, A.S. Kumar and D.S. Gelles (American Society for Testing and Materials, Philadelphia, 1992) p. 749.
- [21] R.E. Stoller, 1996.
- [22] S.J. Zinkle, in *Microstructure of Irradiated Materials*, MRS Symposium Proceedings vol. 373, eds. I.M. Robertson et al. (Materials Research Society, Pittsburgh, 1995) p. 287.
- [23] S.J. Zinkle and L.L. Snead, *Nucl. Instr. Meth. B* 116 (1996) 92.
- [24] S.J. Zinkle and G.P. Pells, *J. Nucl. Mater.* (1997) to be publ.
- [25] R. Sizmann, *J. Nucl. Mater.* 69&70 (1978) 386.
- [26] L.K. Mansur, *J. Nucl. Mater.* 206 (1993) 306.
- [27] J.W. Corbett and J.C. Bourgoin, *IEEE Trans. Nucl. Sci.* NS-18 (1971) 11.
- [28] J.C. Bourgoin and J.W. Corbett, *J. Chem. Phys.* 59 (1973) 4042.
- [29] T. Brudevoll, E.A. Kotomin and N.E. Christensen, *Phys. Rev. B* 53 (1996) 7731.
- [30] E.A. Kotomin, M.M. Kuklja, R.I. Eglitis and A.I. Popov, *Mater. Sci. Eng. B* 37 (1996) 212.
- [31] A. Stashans, E.A. Kotomin and J.-L. Calais, *Phys. Rev. B* 49 (1994) 14854.